



Process of simultaneously fabricating and foaming precursor using frictional heat generated during friction stir welding

Yoshihiko Hangai¹ · Hiromi Morohashi¹ · Yasuhiro Aoki² · Hironao Mitsugi¹ · Hidetoshi Fujii²

Received: 24 January 2022 / Accepted: 4 June 2022 / Published online: 20 June 2022
© The Author(s), under exclusive licence to Springer-Verlag London Ltd., part of Springer Nature 2022

Abstract

Precursor foaming is one of the processes used to produce aluminum (Al) foam. This process fabricates a foamable precursor by mixing a blowing agent powder with solid Al. Then, the fabricated precursor is foamed by heat treatment. In this study, the process of simultaneously fabricating and foaming the precursor was attempted by friction stir welding (FSW). A double-sided FSW was used. Al plates and a blowing agent powder were set in the groove of a steel plate, and the precursor was fabricated using a preceding upper tool. Simultaneously, the fabricated precursor was foamed by pressing and traversing a lower tool from the back of the steel plate slightly behind the upper tool. It was shown that FSW was successfully conducted on Al–Si–Cu ADC12 alloy plates using the upper tool, and the precursor was gradually foamed with the traversal of the lower tool. It was indicated that the blowing agent and stabilization agent powders were thoroughly distributed in the stirred region regardless of the tool traversing rate in the range $v = 30\text{--}50$ mm/min. The tool traversing rate of $v = 30$ mm/min was appropriate for sufficient foaming and to obtain Al foam with good pore structures of the entire Al foam. From these results, it was shown that fabricating of precursor and foaming of the obtained precursor can be simultaneously conducted by FSW in a single process.

Keywords Cellular materials · Friction stir welding · Foaming · Precursor

1 Introduction

Light-weight aluminum (Al) foam has been used in the transportation and construction industries [1–5]. Precursor foaming is one of the processes used to produce Al foam. This process fabricates a foamable precursor by mixing a blowing agent powder with solid Al. Then, the fabricated precursor is foamed by heat treatment. Baumgartner et al. [6] and Duarte and Banhart [7] developed a powder metallurgy (P/M) method for the production of the precursor. They foamed the precursor in an electric furnace. Kitazono et al. [8] developed an accumulative roll-bonding method for fabricating precursors. In this process, Al plates can be used as raw materials. They foamed the precursor using an infrared image furnace. Suzuki et al. [9] developed a casting

method for fabricating the precursor that was then foamed in an electric furnace. In this method, a precursor can be obtained by an inexpensive molten metal method without the use of powder. Duarte et al. [10] demonstrated a continuous foaming line of the precursor fabricated by the P/M method. It was composed of three heating zones of varying temperatures and a cooling sector. The movement of the precursor in an electric furnace was achieved by means of a conveyor belt. This process allows for the mass production of Al foam.

Hangai et al. [11] demonstrated a FSW method for the fabrication of the precursor. The FSW itself was developed as a solid-state process to weld Al plates [12, 13]. In this FSW method, the blowing agent powder was mixed into Al plates during a tool traversal by a strong FSW stirring action. They foamed the precursor in an electric furnace. Several studies have been conducted on fabricating metal foams, whose precursors were fabricated by the FSW method, and the foaming was induced by various heat treatments. Papantoniou et al. [14] fabricated MWCNT-reinforced Al–Mg alloy foam and Nisa et al. [15] fabricated Al₂O₃ added Al–Mg–Si alloy foam, in which the heat treatment was conducted in a laboratory furnace. MWCNT and Al₂O₃

✉ Yoshihiko Hangai
hanhan@gunma-u.ac.jp

¹ Faculty of Science and Technology, Gunma University,
Kiryu 376-8515, Japan

² Joining and Welding Research Institute, Osaka University,
Ibaraki 567-0047, Japan

were introduced with a blowing agent. Shandley et al. [16] demonstrated a flame heating process for fabricating Al–Mg alloy foam, and Hangai et al. [17] demonstrated an optical heating process for fabricating Al–Si–Cu alloy foam, which enabled localized foaming. Azizieh et al. [18] fabricated magnesium foam, in which the heat treatment was conducted in an electric furnace.

Recently, the FSW itself has been applied to the welding of steel plates [19, 20]. Generally, the temperature of the steel plate during FSW exceeds the foaming temperature of the Al precursor because of the frictional heat generated between the FSW tool and the steel plates. Hangai et al. [21, 22] developed a method of foaming precursors with Al–Si–Cu alloy and commercial purity Al, respectively, using the frictional heat generated during the FSW of the steel plate. In this process, a precursor prepared in advance was set in the vicinity of the tool traversing line and the precursor was foamed using the frictional heat generated during the tool traversal.

In this study, the fabrication of the precursor and the foaming of the fabricated precursor were conducted simultaneously by FSW, as shown in Fig. 1. Double-sided FSW [23] was used. As shown in Fig. 1a, the Al plates and a blowing agent powder were set in the groove of the steel plate, and the precursor was fabricated using a preceding upper tool. Simultaneously, as shown in Fig. 1b, the fabricated precursor was foamed by pressing and traversing a lower tool from the back of the steel plate slightly behind the upper tool. The effect of the tool traversing rate on precursor foaming was investigated. The pore structures of the Al foam obtained were observed by X-ray computed tomography (X-ray CT).

2 Experimental procedures

2.1 Traversing of upper and lower tools

Figure 2a shows a photograph of the steel plate used in this study, and Fig. 2b shows the dimensions of the steel plate. An SS400 steel plate of 10 mm thickness, 250 mm length,

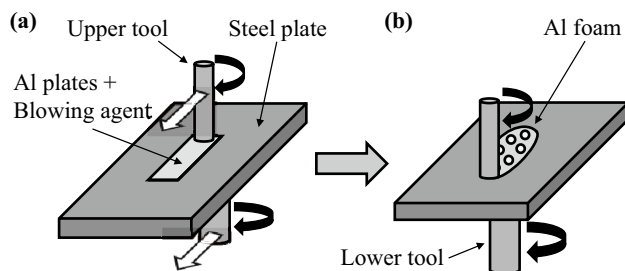


Fig. 1 Schematic illustration of the process of simultaneously fabricating and foaming the precursor by FSW. (a) Set Al plates and a blowing agent powder in a groove of a steel plate. (b) Foaming precursor by traversing tools

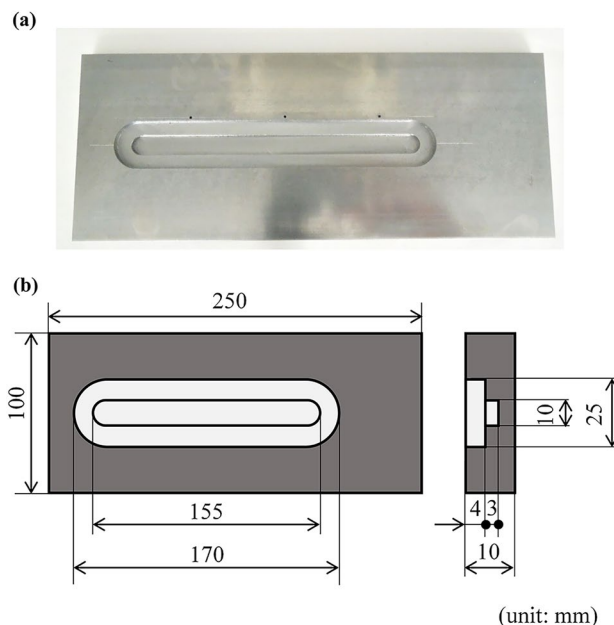
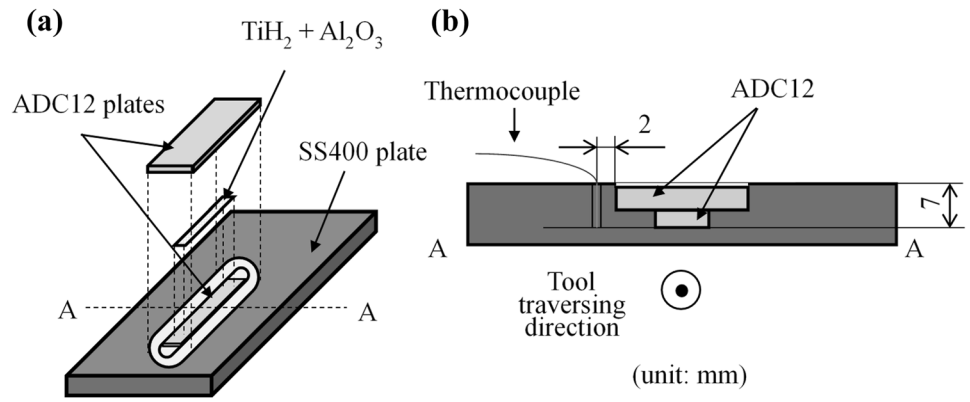


Fig. 2 Dimensions of SS400 plate. (a) Photograph of a steel plate. (b) Dimensions of (a)

and 100 mm width was milled to obtain the stepped groove at the center of the steel plate. The upper groove was at a depth of 4 mm from the surface of the steel plate with a length of 170 mm and a width of 25 mm. The lower groove was milled at a depth of 3 mm from the bottom surface of the upper groove at the center of the upper groove with a length of 155 mm and a width of 10 mm.

Al–Si–Cu alloy, ADC12, high-pressure die-casting plates were used as the precursor material. The liquidus and solidus temperatures of the ADC12 alloy are 580 and 515 °C, respectively [24]. A wide ADC12 plate of 3 mm thickness, 150 mm length, and 25 mm width, and a narrow ADC12 plate of 3 mm thickness, 150 mm length, and 10 mm width were prepared by wire electric discharge machining from ADC12 die casting plates of 3 mm thickness, 210 mm length, and 80 mm width. As shown in Fig. 3, the narrow ADC12 plate was placed into the bottom groove. Then, the mixture of a blowing agent powder (titanium dihydride, TiH_2 , particle diameter below 45 μm) and a stabilization agent powder (α -alumina, $\alpha\text{-Al}_2\text{O}_3$, particle diameter approximately 1 μm) was placed on the narrow ADC12 plate. The amount of TiH_2 powder was 1 wt% and that of Al_2O_3 powder was 5 wt%, in proportion to the weight of the stirred region of the ADC12 plate during the tool traversal. Then, the wide ADC12 plate was placed into the upper groove on the powder mixture. Next, the steel plate with the stacked ADC12 plates in the groove was fixed to an FSW machine by steel bars in accordance with Hangai et al. [21]. The end of the ADC12 plates was also held from above by one of the steel bars. Both upper and lower tools were made of tool steel. The upper tool had a 17 mm shoulder, a height of 4.8 mm,

Fig. 3 Setup of ADC12 plates and powders into the groove of SS400 plate. **(a)** Diagonal view from above. **(b)** Cross-sectional view of A-A in **(a)**

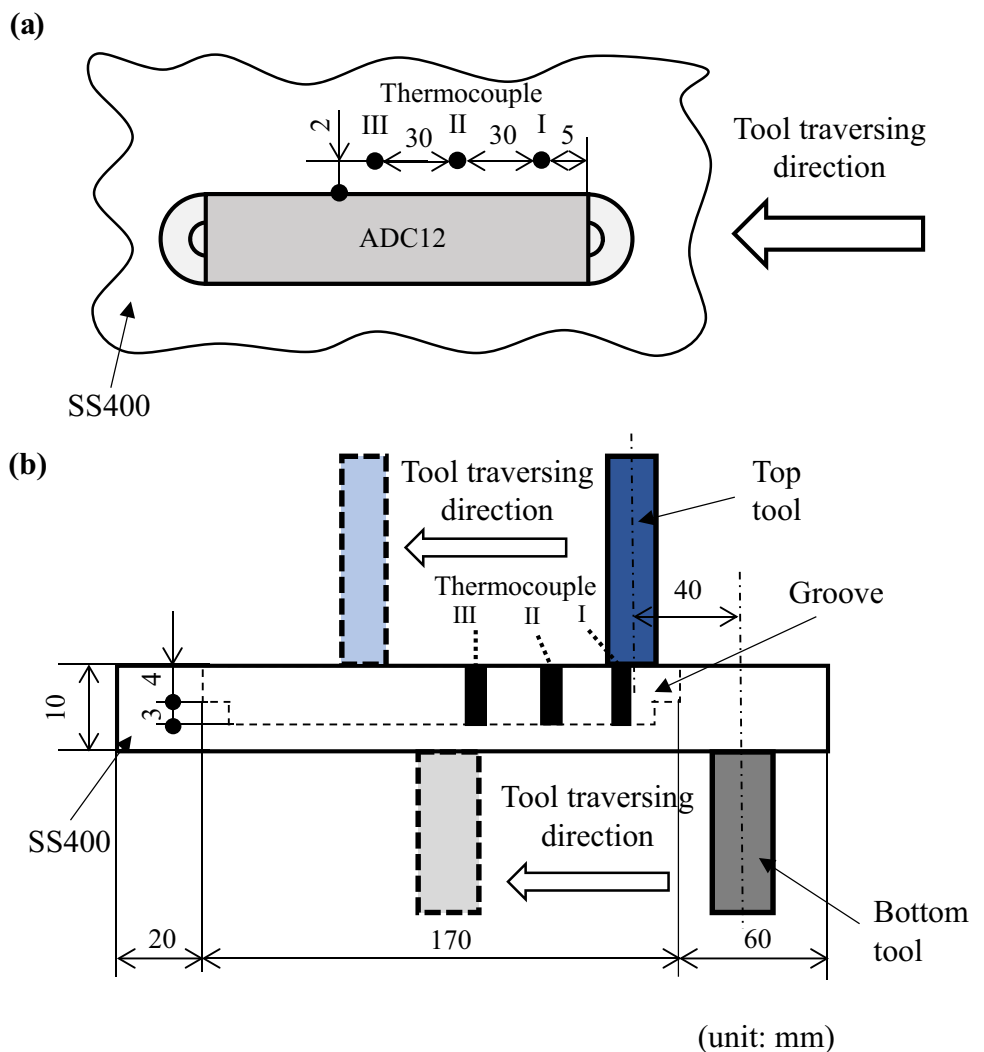


and a 5-mm-diameter probe. The lower tool was a cylinder of 25 mm diameter without a probe. The dimensions of the groove were selected such that the upper tool can traverse without contacting the steel plate during the fabrication of the precursor. A T-shape groove was used because when the width of the lower groove was the same as that of the upper groove, the lower tool broke through the softened steel

plate during the tool traversal because of the strength of the softened steel plate became low. Therefore, the lower groove was made as narrow as possible for the upper tool to traverse without contacting the steel plate.

Figure 4 shows the process of simultaneously fabricating and foaming the precursor by FSW. Temperatures were measured at three locations using K-type thermocouples during the

Fig. 4 Setup of upper and lower tools during the simultaneous process. **(a)** Upper view. **(b)** Side view



tool traversal. The tip of each thermocouple was placed at the same height as the bottom surface of the lower groove. First, the rotating lower tool was pressed onto the steel plate. $t=0$ s was defined as when the lower tool came into contact with the steel plate. Then, the rotating lower tool was held in contact with the steel plate until $t=150$ s for the lower tool to become red hot. The upper tool began to plunge into the ADC12 plates at $t=138$ s at 0.5 mm/s and ended its plunge at $t=150$ s. The distance between the upper tool and the lower tool was kept at 40 mm throughout the experiments. If the distance between the two tools became too small, the ADC12 plates became soft because the temperature of the ADC12 plates was raised by the frictional heat generated by the lower tool. In this case, the powders cannot be stirred into the ADC12 plates thoroughly. Then, both tools started traversing. The center of the upper and lower tools was aligned with that of the ADC12 plates. The rotation rate was 1000 rpm for both tools. The tilt angle was 1° for the lower tool and 3° for the upper tool. The experiments were conducted for tool traversing rates of $v=30$ mm/min, 40 mm/min, and 50 mm/min, respectively.

2.2 Observation of pore structures

The pore structures of the obtained Al foam were observed by X-ray CT. Only the upper part of the Al foam protruding from the steel plate was observed because the Al foam cannot be separated from the steel plate, and X-rays cannot pass through the steel plate. A cone-CT micro focus X-ray system was used. The voltage and current of the X-ray tube were 80 kV and 30 μ m, respectively. The pixel length was 157 μ m/pixel.

3 Experimental results

Figure 5 shows the sequential images of foaming behavior during the traversal of the tools at $v=30$ mm/min. Figure 5a shows an image of the start of the traversal of the upper and

lower tools. Figure 5b shows an image obtained when the lower tool passed directly under thermocouple I. It can be seen that FSW can be successfully conducted on the ADC12 plates using the upper tool without any groove-like defect. In addition, foaming started at the right side of the precursor. Figure 5c–e shows the images obtained when the lower tool passed directly under thermocouples II and III, and at the end of the traversal of the tools, respectively. It can be seen that the precursor was fabricated by the traversal of the upper tool with gradual foaming using the generated heat of the lower tool. Figure 5f shows the temperature history during the traversal of the tools. (a)–(e) in Fig. 5f corresponds to the foaming behavior shown in Figs. 5a–e, respectively. The dotted line shows the liquidus temperature of ADC12 alloy (580 $^\circ$ C). The temperature of thermocouple I, T_I , slightly increased before the traversal of the tools with the transfer of the frictional heat generated between the lower tool and the steel plate. After the tool started traversing at $t=150$ s, T_I was markedly increased by the frictional heat generated between the upper tool and the ADC12 plates. The rate of increase in T_I decreased once after the upper tool passed thermocouple I at around $t=170$ s, then the lower tool approached thermocouple I, and T_I further increased at around $t=220$ s. T_I decreased after the lower tool passed thermocouple I at around $t=250$ s. Hangai et al. [25] demonstrated that the foaming of the ADC12 precursor occurred vigorously above the liquidus temperature of the ADC12 alloy. Since the thermocouple was installed slightly farther from the Al plates and the centers of the tools were aligned with the center of the ADC12 plates, the actual temperature of Al is considered to be slightly higher [21]. Consequently, it is considered that the precursor was heated to above the foaming temperature when the tool reached it. This tendency of T_I was also observed for the temperatures of thermocouple II, T_{II} , and thermocouple III, T_{III} . The maximum temperature gradually increased from thermocouples I to III.

Fig. 5 Foaming behavior and temperature history with $v=30$ mm/min. **a** Start of tool traversal. **b** Lower tool reached thermocouple I. **c** Lower tool reached thermocouple II. **d** Lower tool reached thermocouple III. **e** End of tool traversal. **f** Temperature history during tool traversal

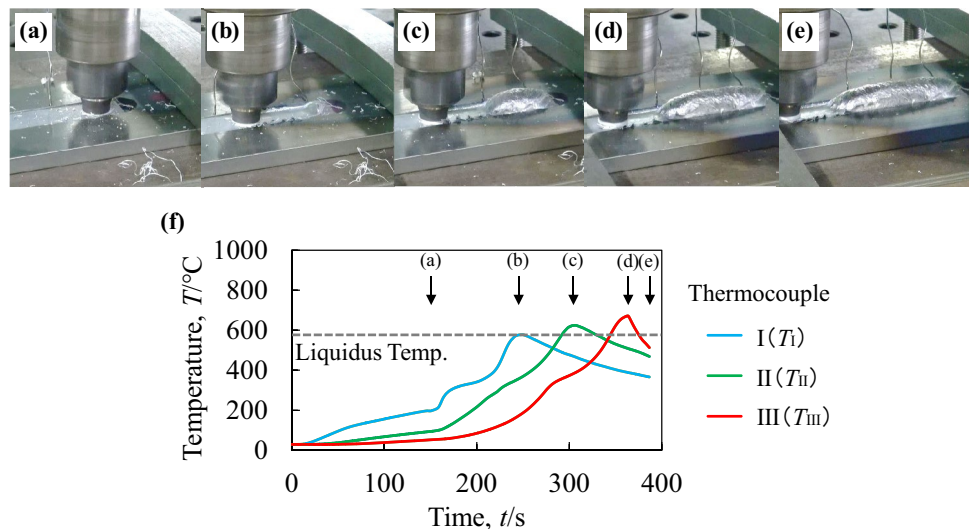
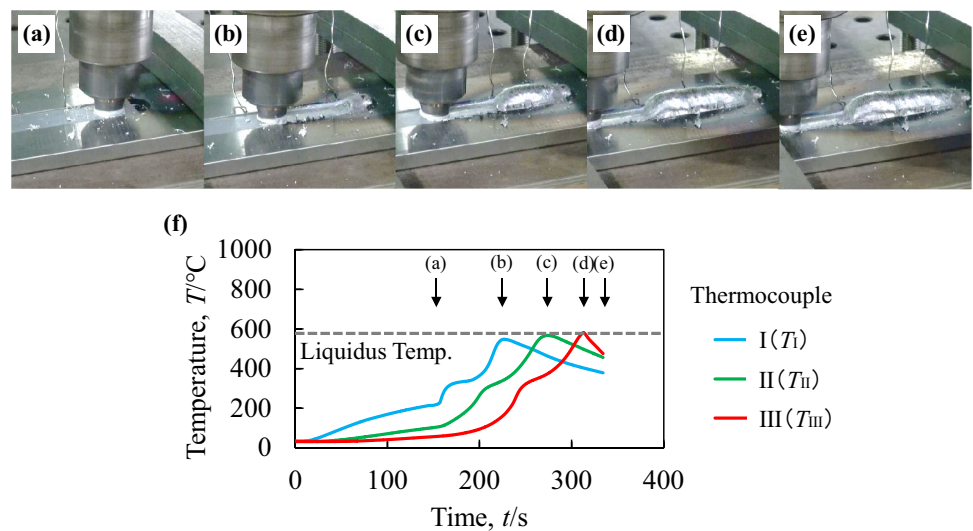


Fig. 6 Foaming behavior and temperature history with $v=40$ mm/min. **a** Start of tool traversal. **b** Lower tool reached thermocouple I. **c** Lower tool reached thermocouple II. **d** Lower tool reached thermocouple III. **e** End of tool traversal. **f** Temperature history during tool traversal



The reason for this is considered to be that heat input was more than heat dissipation for $v=30$ mm/min.

Figure 6 shows the sequential images of foaming behavior during the traversal of the tools at $v=40$ mm/min. Figure 6a–e shows the start of tool traversal, when the lower tool passed directly under thermocouples I, II, and III, and at the end of tool traversal, respectively. It can be seen that FSW was successfully conducted on the ADC12 plates using the upper tool and the precursor was gradually foamed by the traversal of the lower tool even at $v=40$ mm/min. Figure 6f shows the temperature history during the traversal of the tools. A similar tendency as in the case of $v=30$ mm/min was observed, i.e., there are two marked increases in temperature; when the upper tool passed and when the lower tool passed. However, the maximum values of T_I , T_{II} , and T_{III} were lower, and the difference in maximum temperature between T_I , T_{II} , and T_{III} became smaller than those in

the case of $v=30$ mm/min. This is because when v became higher, the amount of heat input became smaller.

Figure 7 shows the sequential images of foaming behavior during the traversal of the tools at $v=50$ mm/min. Figure 7a–e shows the start of tool traversal when the lower tool passed directly under thermocouples I, II, and III, and at the end of tool traversal, respectively. It was shown that FSW was successfully conducted on the ADC12 plates using the upper tool and the precursor was foamed by the traversal of the lower tool even at $v=50$ mm/min. However, foaming was small, and as shown in Fig. 7b, the start of foaming was slightly delayed compared with that in the case of lower v . Figure 7f shows the temperature history during the tool traversal. The temperature during the tool traversal became low. The maximum temperatures of thermocouples I to III were approximately the same, which indicated that heat input was the same as heat dissipation.

Fig. 7 Foaming behavior and temperature history with $v=50$ mm/min. **a** Start of tool traversal. **b** Lower tool reached thermocouple I. **c** Lower tool reached thermocouple II. **d** Lower tool reached thermocouple III. **e** End of tool traversal. **f** Temperature history during tool traversal

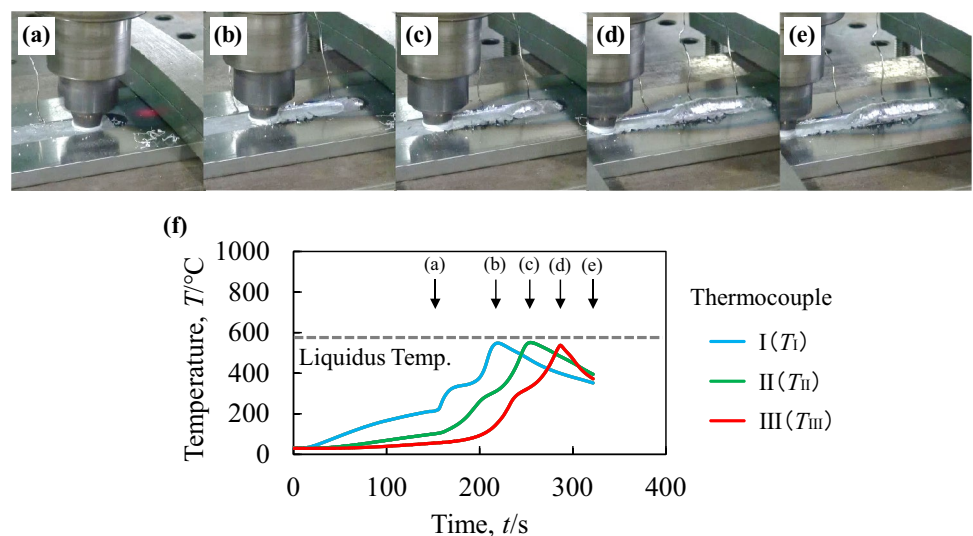


Fig. 8 Obtained Al foam and cross-sectional X-ray CT images

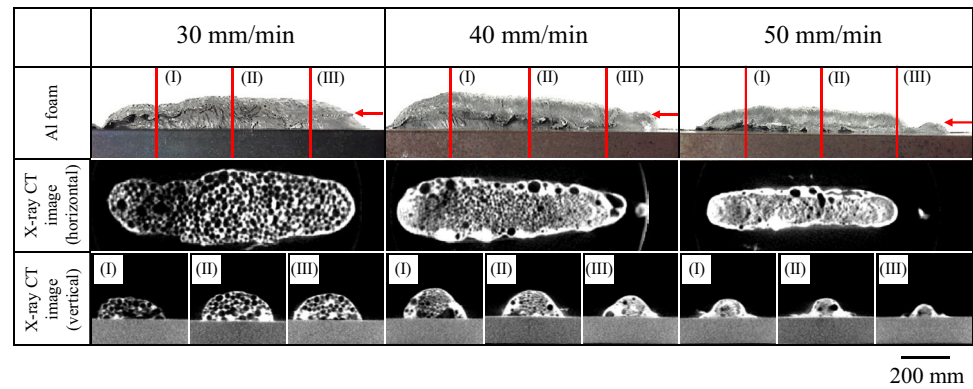


Figure 8 shows the Al foam fabricated at $v=30$, 40, and 50 mm/min observed from the side. The lower part is the steel plate and the upper part is the Al foam. Tool traversal was conducted from right to left. The horizontal cross-sectional X-ray CT images of Al foam at the arrows and the vertical cross-sectional X-ray CT images at (I)–(III) are also shown. White parts indicate Al and black parts indicate pores. It was shown that the Al foam obtained at $v=30$ mm/min has fine pores that are homogeneously distributed. The Al foam obtained at $v=40$ mm/min was also foamed except at the start of tool traversal and at the outer part of the Al foam. A dense part was observed in the Al foam obtained at $v=50$ mm/min. From these results, it was shown that a tool traversing rate of less than $v=40$ mm/min was necessary to foam the precursor, and $v=30$ mm/min was appropriate for sufficient foaming and to obtain Al foam with good pore structures throughout the entire Al foam.

4 Discussion

4.1 Observation of cross section of precursor

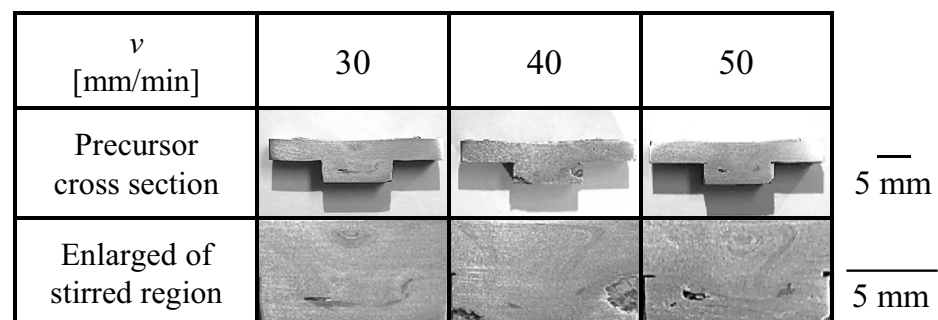
In this study, it was found that Al foam can be obtained by simultaneously fabricating and foaming the precursor by FSW. It was shown that $v=30$ mm/min was appropriate for obtaining Al foam. In this section, the effect of the tool

traversing rate on the mixing of the powders into Al plates is discussed. Figure 9 shows the cross-sectional images of the obtained precursor perpendicular to the tool traversing direction of only the upper tool while the lower tool was not traversed and enlarged images of the stirred region. The precursor was easily removed from the groove of the steel plate. Although small tunnel defects were observed, an onion ring can be observed in the stirred region, which indicated that the blowing agent and stabilization agent powders were thoroughly distributed throughout the stirred region regardless of the tool traversing rate investigated in this study. Hangai et al. [11] demonstrated that when the mixing of the powders was insufficient, the powders were inhomogeneously distributed and remained concentrated between the two Al plates.

4.2 Observation of intermetallic compound (IMC) layer at the interface between Al foam and steel plate

The IMC layer generated between the Al foam and the steel plate was observed whether the heat input into the precursor varied depending on the tool traversing rate. Figure 10 shows the cross-sectional images of the obtained Al foam with part of the steel plate perpendicular to the tool traversing direction around thermocouple II and their backscattered electron (BSE) images at the bottom of the groove in the area within the white dotted boxes indicated by white arrows in the

Fig. 9 Cross-sectional images of precursor and their enlarged images in the vicinity of the stirred region



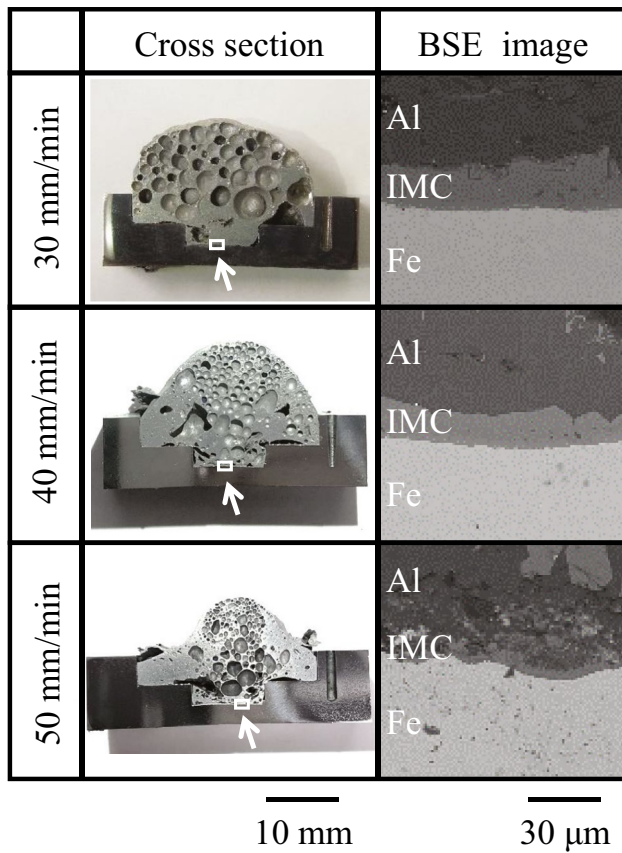


Fig. 10 Cross sections of obtained Al foam around thermocouple II and BSE images around the interface between Al foam and steel plate at the bottom of the groove in the area within white dotted boxes indicated by white arrows in the cross-section

cross-section. From the cross-sectional images, it was shown that pores can be observed approximately throughout the entire region for $v = 30$ mm/min. In contrast, pores became small and the foaming area was limited as v became higher. From the BSE images, an Al–Fe IMC layer was observed at the interface between the Al foam and the steel plate. The IMC layer was observed only at the lower groove wall surface and not at the upper groove wall surface. Therefore, it was indicated that only the lower part of the precursor was heated and the entire precursor was foamed by the transfer of heat within the precursor.

Figure 11 shows the relationship between the tool traversing rate and the thickness of the IMC layer, t_{IMC} , obtained from BSE images. The average and standard deviation of approximately 50 points of t_{IMC} for each Al foam are plotted. It was shown that the IMC layer became thinner as the tool traversing rate became higher, which indicated that the amount of heat input to the precursor decreased and the temperature became lower as the tool traversing rate became higher. Since the precursor fabricated using the upper tool alone can be removed from the steel plate

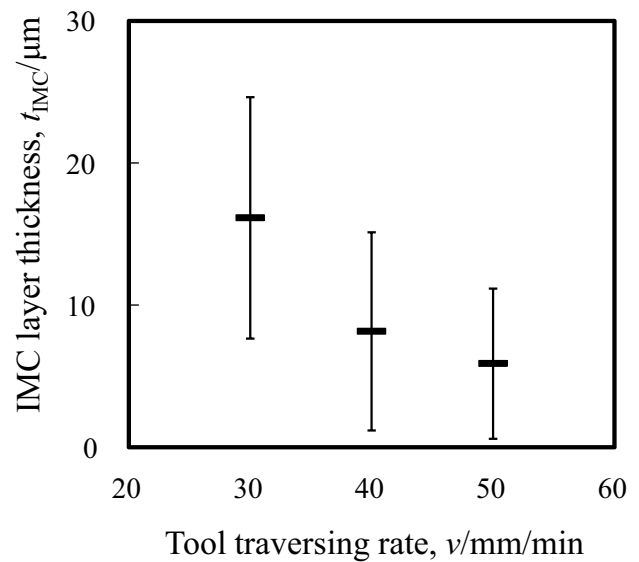


Fig. 11 Relationship between tool traversing rate and IMC layer thickness

after the traversal of the upper tool, it is considered that the precursor and the steel plate were only in close contact during the traversal of the upper tool alone. Then the IMC layer was generated during foaming using the lower tool.

5 Conclusions

In this study, the process of simultaneously fabricating and foaming the precursor was attempted by FSW. A double-sided FSW was used. Al plates and a blowing agent powder were set in the groove of a steel plate, and the precursor was fabricated using a preceding upper tool. Simultaneously, the fabricated precursor was foamed by pressing and traversing a lower tool from the back of the steel plate slightly behind the upper tool. The following conclusions were obtained from the experimental results:

1. FSW was successfully conducted on the ADC12 plates using the upper tool, and the precursor was gradually foamed within the traversal of the lower tool.
2. The tool traversing rate of $v = 30$ mm/min was appropriate for sufficient foaming and to obtain Al foam with good pore structures throughout the entire Al foam.
3. The blowing agent and stabilization agent powders were thoroughly distributed in the stirred region regardless of the tool traversing rate.
4. The amount of heat input into the precursor decreased, and the temperature became lower as the tool traversing rate became higher.

Acknowledgements This work was partly performed under the Cooperative Research Program of the Institute for Joining and Welding Research Institute, Osaka University.

Author contribution Yoshihiko Hangai: methodology and writing—original draft; Hiromi Morohashi and Yasuhiro Aoki: investigation and analysis; Hironao Mitsugi: investigation and visualization; Hidetoshi Fujii: supervision and writing—review and editing.

Funding This work was financially supported partly by JST-Mirai Program grant number JPMJMI19E5, Japan.

Data availability The raw/processed data required to reproduce these findings cannot be shared at this time as the data also forms part of an ongoing study.

Code availability Not applicable.

Declarations

Ethics approval Not applicable.

Consent to participate Not applicable.

Consent for publication Not applicable.

Competing interests The authors declare no competing interests.

References

- Banhart J (2001) Manufacture, characterisation and application of cellular metals and metal foams. *Prog Mater Sci* 46(6):559–632
- García-Moreno F (2016) Commercial applications of metal foams: their properties and production. *Materials* 9(2):85
- Wan T, Liu Y, Zhou C, Chen X, Li Y (2021) Fabrication, properties, and applications of open-cell aluminum foams: a review. *J Mater Sci Technol* 62:11–24. <https://doi.org/10.1016/j.jmst.2020.05.039>
- Kumar N, Bharti A (2021) Review on powder metallurgy: a novel technique for recycling and foaming of aluminium-based materials. *Powder Metall Met Ceram* 60(1–2):52–59. <https://doi.org/10.1007/s11106-021-00214-4>
- Parveez B, Jamal NA, Maleque A, Yusof F, Jamadon NH, Adzila S (2021) Review on advances in porous Al composites and the possible way forward. *J Mater Res Technol* 14:2017–2038. <https://doi.org/10.1016/j.jmrt.2021.07.055>
- Baumgartner F, Duarte I, Banhart J (2000) Industrialization of powder compact foaming process. *Adv Eng Mater* 2(4):168–174. [https://doi.org/10.1002/\(sici\)1527-2648\(200004\)2:4%3c168::aid-adem168%3e3.3.co;2-f](https://doi.org/10.1002/(sici)1527-2648(200004)2:4%3c168::aid-adem168%3e3.3.co;2-f)
- Duarte I, Banhart J (2000) A study of aluminium foam formation - kinetics and microstructure. *Acta Mater* 48(9):2349–2362
- Kitazono K, Sato E, Kuribayashi K (2004) Novel manufacturing process of closed-cell aluminum foam by accumulative roll-bonding. *Scr Mater* 50(4):495–498. <https://doi.org/10.1016/j.scriptamat.2003.10.035>
- Suzuki R, Nishimoto T, Hangai Y, Shoji I, Matsubara M (2018) Fabrication of aluminum foam by casting precursor method. *J Jpn Inst Met Mater* 82(9):349–357
- Duarte I, Vesjenak M, Vide MJ (2019) Automated continuous production line of parts made of metallic foams. *Metals* 9(5):531. <https://doi.org/10.3390/met9050531>
- Hangai Y, Utsunomiya T, Hasegawa M (2010) Effect of tool rotating rate on foaming properties of porous aluminum fabricated by using friction stir processing. *J Mater Process Technol* 210(2):288–292. <https://doi.org/10.1016/j.jmatprotec.2009.09.012>
- Thomas WM, Nicholas ED (1997) Friction stir welding for the transportation industries. *Mater Des* 18(4–6):269–273. [https://doi.org/10.1016/s0261-3069\(97\)00062-9](https://doi.org/10.1016/s0261-3069(97)00062-9)
- Mishra RS, Ma ZY (2005) Friction stir welding and processing. *Mater Sci Eng R-Rep* 50(1–2):1–78. <https://doi.org/10.1016/j.mser.2005.07.001>
- Papantoniou IG, Kyriakopoulou HP, Pantelis DI, Manolakos DE (2018) Fabrication of MWCNT-reinforced Al composite local foams using friction stir processing route. *Int J Adv Manuf Technol* 97(1–4):675–686. <https://doi.org/10.1007/s00170-018-1964-3>
- Nisa SU, Pandey S, Pandey PM (2021) Significance of Al₂O₃ addition in the aluminum 6063 metal foam formation through friction stir processing route - a comprehensive study. *Proc Inst Mech Eng Part L-J Mater Des Appl* 235(12):2737–2745. <https://doi.org/10.1177/14644207211034531>
- Shandley R, Maheshwari S, Siddiquee AN, Mohammed S, Chen DL (2020) Foaming of friction stir processed Al/MgCO₃ precursor via flame heating. *Mater Res Express* 7(2). <https://doi.org/10.1088/2053-1591/ab6ef0>
- Hangai Y, Amagai K, Omachi K, Tsurumi N, Utsunomiya T, Yoshikawa N (2018) Forming of aluminum foam using steel mesh as die during foaming of precursor by optical heating. *Opt Laser Technol* 108:496–501. <https://doi.org/10.1016/j.optlastec.2018.07.016>
- Azizieh M, Pourmansouri R, Balak Z, Kafashan H, Mazaheri M, Kim HS (2017) The application of friction stir processing to the fabrication of magnesium-based foams. *Arch Metall Mater* 62(4):1957–1962. <https://doi.org/10.1515/amm-2017-0293>
- Fujii H, Cui L, Tsuji N, Maeda M, Nakata K, Nogi K (2006) Friction stir welding of carbon steels. *Mater Sci Eng A* 429(1–2):50–57. <https://doi.org/10.1016/j.msea.2006.04.118>
- Heidarzadeh A, Mironov S, Kaibyshev R, Cam G, Simar A, Gerlich A, Khodabakhshi F, Mostafaei A, Field DP, Robson JD, Deschamps A, Withers PJ (2021) Friction stir welding/processing of metals and alloys: a comprehensive review on microstructural evolution. *Prog Mater Sci*. <https://doi.org/10.1016/j.pmatsci.2020.100752>
- Hangai Y, Takada K, Endo R, Fujii H, Aoki Y, Utsunomiya T (2018) Foaming of aluminum foam precursor during friction stir welding. *J Mater Process Technol* 259:109–115. <https://doi.org/10.1016/j.jmatprotec.2018.04.016>
- Hangai Y, Takada K, Fujii H, Aoki Y, Aihara Y, Nagahiro R, Amagai K, Utsunomiya T, Yoshikawa N (2020) Foaming of A1050 aluminum precursor by generated frictional heat during friction stir processing of steel plate. *Int J Adv Manuf Technol* 106(7):3131–3137. <https://doi.org/10.1007/s00170-019-04834-4>
- Chen J, Fujii H, Sun Y, Morisada Y, Ueji R (2013) Fine grained Mg–3Al–1Zn alloy with randomized texture in the double-sided friction stir welded joints. *Mater Sci Eng A* 580:83–91. <https://doi.org/10.1016/j.msea.2013.05.044>
- The-Japan-Institute-of-Light-Metals (1991) Structures and properties of aluminum. The Japan Institute of Light Metals, Tokyo
- Hangai Y, Amagai K, Tsurumi N, Omachi K, Shimizu K, Akimoto K, Utsunomiya T, Yoshikawa N (2018) Forming of aluminum foam using light-transmitting material as die during foaming by optical heating. *Mater Trans* 59(11):1854–1859. <https://doi.org/10.2320/matertrans.M2018218>

Publisher's Note Springer Nature remains neutral with regard to jurisdictional claims in published maps and institutional affiliations.